

Raman association of H₂ in the early universe

Mark P. J. van der Loo,[†] Gerrit C. Groenenboom,[†] Michael J. Jamieson[‡] and Alex Dalgarno

Received 29th November 2005, Accepted 6th February 2006

First published as an Advance Article on the web

DOI: 10.1039/b516803a

We investigate the contribution made by Raman scattering to the formation of molecular hydrogen in astrophysical environments characteristic of the early stages of the evolution of the universe. In the Raman process that we study, a photon is scattered by a pair of colliding hydrogen atoms leaving a hydrogen molecule that is stabilized by the transfer of kinetic and binding energy to the photon. We use a formulation for calculating the photon scattering cross section in which an infinite sum of matrix elements over rovibrational levels of dipole accessible electronic states is replaced by a single matrix element of a Green's function. We evaluate this matrix element by using a discrete variable representation.

1. Introduction

The formation of molecules was an important event in the evolution of the early universe. The chemistry and formation of molecules in the early universe have been reviewed recently by Lepp *et al.*,¹ Dalgarno,² and Galli and Palla.³ The presence of molecular hydrogen is believed to have played an important role in the early cosmological structure formation.⁴

The mechanisms that have been explored for the formation of molecular hydrogen are the reaction sequences initiated by the radiative association of H⁺ and He and H⁺ and H and the direct formation of H₂ by associative detachment in collisions of H⁻ and H and the radiative association of ground and excited hydrogen atoms. In this paper we focus on the formation of hydrogen molecules from hydrogen atoms. Symmetry arguments show that direct association of a pair of ground state hydrogen atoms to form a hydrogen molecule which is stabilised by the emission of a photon is not possible; the symmetry is broken for a collision of a hydrogen atom and a deuterium atom and direct association can proceed slowly.^{3,5,6} We investigate the possibility that a contribution to the formation of molecular hydrogen in astrophysical environments arises from Raman scattering of photons where a transition occurs from a point in the vibrational continuum of the ground electronic state, X¹Σ_g⁺, of molecular hydrogen (that describes a pair of colliding hydrogen atoms) to a bound vibrational level of the X¹Σ_g⁺ state; the excess energy (kinetic and binding) is removed by the scattered photons. When the incident photon has a large wavelength, the scattering cross section and corresponding rate of association for the production of molecular hydrogen can be calculated from the polarizability of the hydrogen molecule.^{7,8} However, at wavelengths close to and smaller than Lyman α, resonant excitation of the bound rovibrational levels of dipole accessible excited electronic states of the molecule enhances the cross sections and association rates.⁸

Harvard-Smithsonian Center for Astrophysics, 60 Garden Street, Cambridge MA 02138, USA

[†] Permanent Address: Institute of Theoretical Chemistry, University of Nijmegen, Toernooiveld 1 6525 ED Nijmegen, The Netherlands.

[‡] Permanent Address: Department of Computing Science, University of Glasgow, 17 Lilybank Gardens, Glasgow, UK G12 8QQ.

2. Theory

The Raman association process involves the inelastic scattering, from energy $\hbar\omega$ to $\hbar\omega_{sc}$, of electromagnetic radiation by a pair of hydrogen atoms colliding on the $X^1\Sigma_g^+$ ground state surface of molecular hydrogen:



The cross section in $\text{cm}^2 \text{J}^{-1}$ associated with this process is given by:

$$\sigma_{fi}(\omega) = \frac{8\pi\alpha^2\omega\omega_{sc}^3}{9c^2e^4} S_{fi}(\omega), \quad (2)$$

where α is the fine-structure constant, c is the speed of light and e is the electronic charge. In eqn (2) the Raman scattering matrix $S_{fi}(\omega)$ is given by the Kramers–Heisenberg equation:⁹

$$S_{fi}(\omega) = \sum_{st} \left| \sum_m \frac{\langle f | \hat{\mu}_s | m \rangle \langle m | \hat{\mu}_t | i \rangle}{\omega_{mi} - \omega + i\Gamma_m/2} + \frac{\langle f | \hat{\mu}_s | m \rangle \langle m | \hat{\mu}_t | i \rangle}{\omega_{mi} + \omega} \right|^2, \quad (3)$$

where the coherent sum is over all the intermediate states $|m\rangle$, $\omega_{mi} = \omega_i - \omega_m$, Γ_m is the inverse lifetime of the intermediate state $|m\rangle$ and $\hat{\mu}_s$ and $\hat{\mu}_t$ are components of the dipole moment operator. In the calculation of Federman and Frommhold⁸ the sum over intermediate states in eqn (3) was evaluated explicitly but only partially. The sum may be evaluated implicitly in terms of dipole response functions^{10–15} which may be expressed in terms of Green's functions.^{13,14} We discuss below a method to evaluate the matrix elements of the Green's functions. The first term in eqn (3) can give rise to resonances where the second term can be neglected. In the off-resonant case, where $\omega_{mi} \gg \omega$, the scattering matrix is given by the polarizability theory of Placzek and Teller⁷ as

$$S_{fi}^{PT}(\omega) = \frac{1}{9} |\langle f | \alpha_{\parallel} + 2\alpha_{\perp} | i \rangle|^2 \delta_{J''J'} + B_{J''}^{J'} |\langle f | \alpha_{\parallel} - \alpha_{\perp} | i \rangle|^2, \quad (4)$$

where α_{\parallel} and α_{\perp} are the parallel and perpendicular components, respectively, of the polarizability of a hydrogen molecule in its ground state, and $B_{J''}^{J'}$ depends on the initial and final rotational quantum numbers (J'' and J' , respectively) of the system

$$B_{J''}^{J'} = \begin{cases} \frac{3}{2} \frac{J''(J''-1)}{(2J''-1)(2J''+1)} & J' = J'' - 2 \\ \frac{J''(J''+1)}{(2J''-1)(2J''+3)} & J' = J'' \\ \frac{3}{2} \frac{(J''+1)(J''+2)}{(2J''+1)(2J''+3)} & J' = J'' + 2. \end{cases} \quad (5)$$

We apply the usual Born–Oppenheimer approximation and we represent the wave functions in eqn (3) in the Hund's case (a) basis $\{|\psi_{(ap)}^{JM_J}\rangle\}$ as

$$|\psi_{(ap)}^{JM_J}\rangle = \frac{1 + (-1)^p \hat{i}}{\sqrt{2 + 2\delta_{A0}\delta_{\Sigma 0}}} \sqrt{[J]/4\pi} D_{M_J\Omega}^{(J)*}(\alpha, \beta, 0) |v; nAS\Sigma\rangle, \quad (6)$$

where A , S , Σ , and Ω are the usual Hund's case (a) quantum numbers, p denotes parity, \hat{i} is the parity operator, n is the electronic primary quantum number, $\sqrt{[J]/4\pi} D_{M_J\Omega}^{(J)*}(\alpha, \beta, 0)$ is a two-angle normalized Wigner D function, and v the vibrational quantum number, which is replaced by the kinetic energy E for continuum states. We use the parity convention defined by van Vroonhoven and Groenenboom.¹⁶ We denote $2J + 1$ by $[J]$ throughout.

Neglecting the second term in eqn (3) and integrating over the angular variables we find that the rotationally resolved scattering matrix for relative collision energies E'' in the parity-unadapted basis can be written as

$$S_{J',\nu'\Omega';J'',E''\Omega''}(\omega) = \frac{1}{[J'']} \sum_{M_J'' M_{J'}} \left| \sum_{J\Omega} S_{J' M_{J'} \Omega'}^{J'' M_J'' \Omega''} (J\Omega) M_{\nu' J' \Omega'}^{E'' J'' \Omega''} (J\Omega) \right|^2. \quad (7)$$

The angular factor S is given by

$$S_{J' M_{J'} \Omega'}^{J'' M_{J''} \Omega''}(J\Omega) = (-1)^{J+\Omega+J'-M_{J'}+J-M_J} [J] \sqrt{[J'] [J'']} \sum_{M_J} \begin{pmatrix} J' & 1 & J \\ -M_{J'} & 0 & M_J \end{pmatrix} \\ \times \begin{pmatrix} J & 1 & J'' \\ -M_J & 0 & M_{J''} \end{pmatrix} \begin{pmatrix} J' & 1 & J \\ 0 & -\Omega & \Omega \end{pmatrix} \begin{pmatrix} J & 1 & J'' \\ -\Omega & \Omega & 0 \end{pmatrix},$$

where we used the fact that in the $X^1\Sigma_g^+$ state we have $\Omega' = \Omega'' = 0$.

The angular factor predicts electronic and rotational selection rules for the Raman association process, schematically represented in Fig. 1; the selection rules also reduce the number of candidates in the coherent sum over intermediate states in eqn (3). In Raman association, the system starts in the continuum of levels with rotational quantum number J'' of the $X^1\Sigma_g^+$ ground electronic state and finishes as a bound level, with rotational quantum number J'' or $J'' \pm 2$, of the $X^1\Sigma_g^+$ electronic state; transitions to final levels with rotational quantum number $J'' \pm 1$ are forbidden. Fig. 1 signifies that the only allowed intermediate states in eqn (3) are levels of electronic states of $^1\Sigma_u^+$ and $^1\Pi_u$ symmetries, and that the rotational quantum numbers are restricted to $J'' \pm 1$ for the $^1\Sigma_u^+$ intermediate levels and J'' and $J'' \pm 1$ for the $^1\Pi_u$ intermediate levels. The dynamical part M is given by:

$$M_{v' J' \Omega'}^{E'' J'' \Omega''}(J\Omega) = \hbar \sum_n \langle v'; J' n' \Omega' | \hat{d}_{-\Omega} \hat{G}_{nJ\Omega} \hat{d}_{\Omega} | E''; J'' n'' \Omega'' \rangle_r, \quad (9)$$

where integration is over the nuclear coordinate r , the \hat{d}_x are the relevant components of the body-fixed dipole operator given by $\hat{\mu}_s = \sum_x \hat{d}_x D_{sx}^{(1)*}(\alpha, \beta, 0)$, and \hat{G} is the Green operator associated with the Schrödinger equation for nuclear motion in the adiabatic Born–Oppenheimer hydrogen atom r -dependent potential, $V_{n\Omega}(r)$, of the relevant electronic intermediate state

$$\hat{G}_{nJ\Omega}(\omega) = \left[E'' + \hbar\omega - \left(\frac{-\hbar^2}{2\mu r} \frac{d^2}{dr^2} r + V_{n\Omega}(r) + \frac{f^\Omega(J)}{2\mu r^2} \right) + i\Gamma/2 \right]^{-1}, \quad (10)$$

where r is the nuclear separation, μ is the reduced mass for the motion and

$$f^\Omega(J) = \begin{cases} J(J+1) & \Omega = 0 \\ J(J+1) - 1 & |\Omega| = 1. \end{cases} \quad (11)$$

Here we have neglected terms in the Hamiltonian that couple different electronic states.

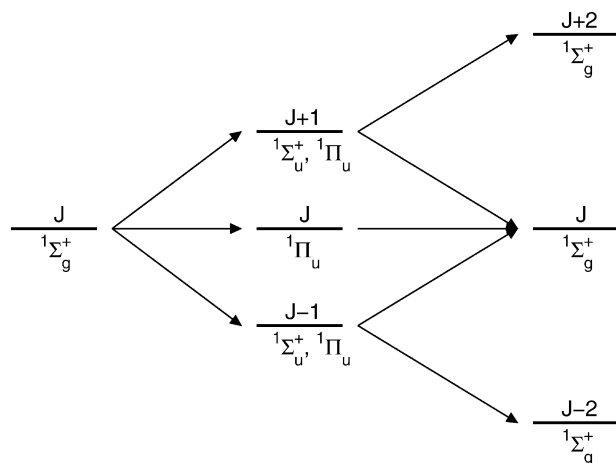


Fig. 1 The possible pathways for rotational changes in Raman association. The path $J \rightarrow J \rightarrow J$ is not possible for $^1\Sigma_u^+$ intermediate states.

In practice, the infinite sum over electronic states in eqn (3) is truncated so as not to include any contributions from distant electronic states. However the contribution of distant electronic states to the scattering matrix can be considered to be independent of ω .¹⁵ We write

$$S_{fi}(\omega) = S_{fi}^{KH}(\omega) + S_{fi}^{\text{corr}}, \quad (12)$$

where S_{fi}^{KH} is the scattering matrix element obtained when the sum in eqn (3) is truncated and S_{fi}^{corr} is a constant correction term that accounts for the distant states' contribution which can be estimated by examining scattering matrix elements in the off-resonance region, where the Placzek–Teller approximation holds. The correction is

$$S_{fi}^{\text{corr}} = S_{fi}^{PT}(\omega) - S_{fi}^{KH}(\omega) \quad \omega \ll \omega_{mi}, \quad (13)$$

where S_{fi}^{PT} is expressed in terms of the polarizabilities, α_{\perp} and α_{\parallel} , by eqn (4) and the calculation of the polarizabilities includes all intermediate electronic states. We evaluate the correction from eqn (13) with $S_{fi}^{PT}(\omega)$ and $S_{fi}^{KH}(\omega)$ computed at energy $\hbar\omega = 2.401 \times 10^4 \text{ cm}^{-1}$.

In the calculation by Federman and Frommold,⁸ the term $\alpha_{\parallel} + 2\alpha_{\perp}$ of eqn (4) was replaced by $\alpha_{\parallel} + 2\alpha_{\perp} - 6\alpha_0$, where α_0 is the polarizability of the hydrogen atom. Similarly, the r -dependent dipole transition moments $d(r)$ were replaced by $d(r) - d(\infty)$. However, since nuclear eigenstates on the $X^1\Sigma_g^+$ electronic surface are orthogonal, the extra term $\langle f|\alpha_0|i\rangle$, arising from the subtraction, vanishes and is therefore unnecessary for rovibrational Raman scattering.

3. Numerical methods

The central part of our calculation is the evaluation of eqn (13). We choose a grid-based representation. The nuclear Hamiltonian matrix and final nuclear bound states are represented using the sinc-function discrete variable representation (sinc-DVR).¹⁷ The numerical initial state nuclear wave functions are obtained by using the renormalized Numerov method to propagate them on the $X^1\Sigma_g^+$ potential energy curve and then matching them to scattering boundary conditions. We restrict the sum over intermediate electronic states to a sum over 6 optically allowed states; 3 are of $^1\Sigma_u^+$ symmetry and 3 are of $^1\Pi_u$ symmetry (see Fig. 2). The *ab initio* potential energy curves and electronic dipole transition moments are taken from calculations by Wolniewicz and Staszewska.^{18–21} We use the vibrationally resolved lifetimes from the work by Fantz and Wunderlich²² to estimate the inverse lifetime Γ_m of each intermediate state. In the case where $E'' + \hbar\omega > V_{n\Omega}(r \rightarrow \infty)$, that is,

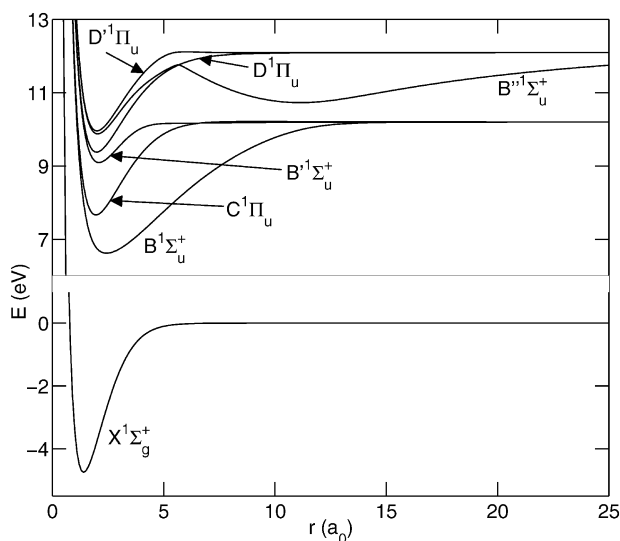


Fig. 2 The lowest singlet potential energy curves^{18–21} of H_2 ; the $B'^1\Sigma_u^+$ and the $D'^1\Pi_u$ states each have a double well structure.

where the sum of the initial state energy and the energy of the incoming photon exceeds the dissociation limit of an intermediate electronic state, we use the Green function absorbing boundary condition (ABC) method^{23–25} to prevent the matrix in eqn (10) from becoming singular. The ABC method consists of replacing the constant $\frac{1}{2}\Gamma_m$ by an r -dependent function $\gamma(r)$, thus effectively augmenting the potential $V_{n\Omega}(r)$ with a negative imaginary potential which absorbs the wave function in the physically non-relevant outer region. Here we choose the Woods–Saxon potential

$$\gamma(r) = \frac{2\lambda}{1 + \exp(r_{\max} - r)/\eta)}, \quad (14)$$

where λ and r_{\max} values are chosen such that sufficient absorption takes place and η is chosen to be small enough to ensure that no significant reflection occurs.

The main computational task is to solve the linear systems of equations associated with the representation of the term $\hat{G}_{nJ\Omega} \hat{d}_{\Omega} |E''; J'' n'' \Omega\rangle$ in eqn (9). Since the potential energy curves of intermediate electronic states have different r -dependences, we save computational time by adapting the grid and minimizing the number of basis functions for each intermediate state. That is, we keep the grid spacing constant and minimize the range of the grid. The linear systems can then be solved on each grid separately, and the solutions projected so that the inner product with the final state $\langle v; J' n' \Omega' | \hat{d}_{-\Omega}$ can be taken. Table 1 shows the different grids used in this work. At these resonances the matrix in eqn (10) is singular and we represent the term $\hat{G}_{nJ\Omega} \hat{d}_{\Omega} |E''; J'' n'' \Omega\rangle$ in eqn (9) by $\chi_v^{nJ\Omega}(r) \langle v; nJ\Omega | d_{\Omega} |E''; n'' J'' \Omega'' \rangle / (i\Gamma_m/2)$, where $\chi_v^{nJ\Omega}(r)$ is the rovibrational nuclear wave function associated with the resonance. Inspection of the resonances shows that the two methods of calculation are consistent with each other.

The Raman association cross section is computed for a grid of photon frequencies. Because the cross section is very sharply peaked around resonances we do not use a grid that is linear in photon energy $\hbar\omega$ but choose instead a grid that is logarithmically spaced around each resonance. The grid is cut off at 13.6 eV. Extensive experimentation showed that choosing 50 logarithmically spaced points around every resonance while leaving out redundant points gives a satisfactory description of the spectral features. In total there are about 350 rovibrational resonances in each spectrum depending on the initial rotational quantum number, yielding about 12 300 points on average to be computed per spectrum.

For comparison we compute cross sections according to the theory of Placzek and Teller. The matrix elements in eqn (4) are evaluated using the r -dependent polarizability of molecular hydrogen in the ground state computed by Wolniewicz.²¹ The initial (scattering) and final (bound) states are evaluated on the grid as described above.

4. Results

Fig. 3 shows the total Raman association cross section as a function of photon energy for two hydrogen atoms, colliding at an energy of $E = 0.448$ eV. The cross section shown is computed with the truncated Kramers–Heisenberg equation, and the corrections from eqn (12) and (13) are applied. The (initial) rotational quantum number is $J'' = 6$; this is appropriate to the most abundant rotational state in the early universe at a matter and radiation temperature of about 4000 K. The bars show where rovibrational resonances of the various intermediate states occur. The cross section increases smoothly with photon energy, until the resonance region is reached. At higher photon energies, in the resonance region, the cross section increases significantly. The off-resonance background cross section increases by about four orders of magnitude compared with the low photon energy region. At a resonance, the cross section may be five to ten orders of magnitude larger than the background cross section. At about $78\,770\text{ cm}^{-1}$ the cross section in this spectrum decreases rapidly. The reason is that at these photon energies the second dissociation continuum of

Table 1 Number of grid points used for each intermediate state potential. The grid points are given by 0.2, 0.3, . . . , $0.2 + 0.1N$

	$X^1\Sigma_g^+$	$B^1\Sigma_u^+$	$B'^1\Sigma_u^+$	$B''^1\Sigma_u^+$	$C^1\Pi_u$	$D^1\Pi_u$	$D'^1\Pi_u$
N	118	198	198	398	118	198	398

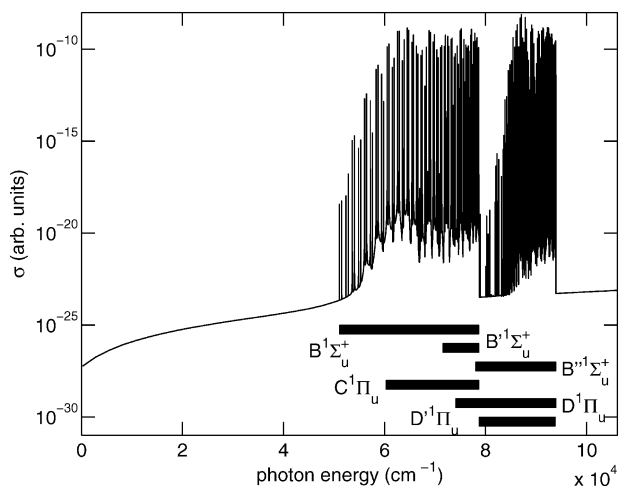


Fig. 3 Raman association cross section for hydrogen atoms colliding with a relative collision energy of 0.448 eV with $J'' = 6$. The bars indicate where rovibrational resonances of the indicated electronic states are found.

the $B^1\Sigma_u^+$, $B'^1\Sigma_u^+$, and $C^1\Pi_u$ states is reached, and there are not many bound state resonances in this energy region. At higher energies the number of resonances, and thus the cross section, increases significantly again. The sharp cutoff at $93\,950\text{ cm}^{-1}$ occurs where the sum of the photon energy and the collision energy exceeds the dissociation limit of the $B'^1\Sigma_u^+$, $D^1\Pi_u$, and $D'^1\Pi_u$ states.

In Fig. 4 we show the resonances associated with intermediate states, specifically the $v = 0, J = 5$, and $v = 0, J = 7$ levels of the $B^1\Sigma_u^+$ electronic state; absence of a resonance at the $v = 0, J = 6$ level is consistent with the selection rules depicted in Fig. 1. The dashed lines indicate the cross sections, $\sigma_{J' \leftarrow J''} \equiv \sum_{v'} \sigma_{v' J' : E'' J''}$, associated with transitions from an initial state whose rotational quantum number is $J'' = 6$ in the $X^1\Sigma_g^+$ continuum to the various final rovibrational levels of the $X^1\Sigma_g^+$ state. In the $\sigma_{6 \leftarrow 6}$ cross section we find the two resonances at the $v = 0, J = 5$ and $v = 0, J = 7$ levels of the $B^1\Sigma_u^+$ state, showing the contributions *via* the two paths for the intermediate $^1\Sigma_u^+$ electronic state

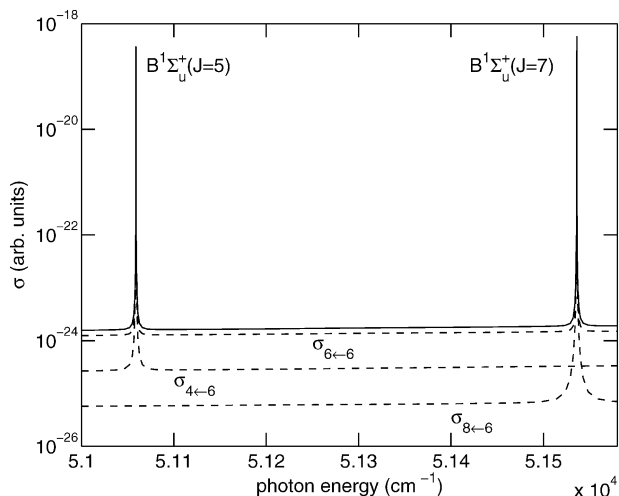


Fig. 4 Raman association cross sections at the resonances associated with the $B^1\Sigma_u^+(v = 0), J = 5$ and $J = 7$ states. The dashed lines indicate the cross sections for the $J' = 4 \leftarrow J'' = 6$, $J' = 6 \leftarrow J'' = 6$ and $J' = 8 \leftarrow J'' = 6$ transitions, respectively.

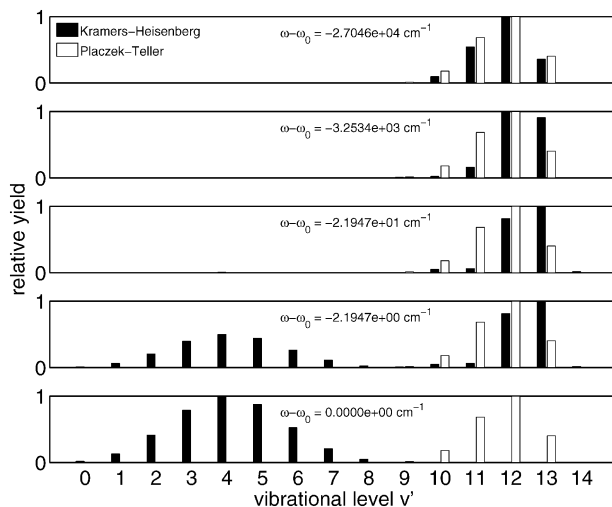


Fig. 5 Relative yield of $X^1\Sigma_g^+$ vibrational states upon Raman association of H atoms, colliding with a relative collision energy of 0.448 eV and $J'' = 6$ as a function of photon angular frequency ω . Here, ω_0 is the frequency associated with the $B^1\Sigma_u^+(v = 0, J = 5)$ resonance.

depicted in Fig. 1. We find one resonance in each of the $\sigma_{4\leftarrow 6}$ and $\sigma_{8\leftarrow 6}$ cross sections associated, respectively, with the $v = 0, J = 5$ and $v = 0, J = 7$ levels of the $B^1\Sigma_u^+$ state.

We also calculated the vibrationally resolved cross sections $\Sigma_{J''\sigma_{v'J''\leftarrow E''J''}}$. In Fig. 5 the relative vibrational distributions at different photon scattering energies, $\hbar\omega$, are compared. The black bars indicate results obtained with the Kramers–Heisenberg formula, eqn (3), and the white bars indicate results obtained from the Placzek–Teller approximation. The photon angular frequencies are presented relative to the position of the angular frequency, denoted ω_0 , of the $B^1\Sigma_u^+(v = 0, J = 5)$ resonance. In the off-resonance region, where $\omega - \omega_0$ is equivalent to an energy shift from resonance of about $-40\,265\text{ cm}^{-1}$ (and $\hbar\omega = 2.401 \times 10^4\text{ cm}^{-1}$), the vibrational distributions predicted by the Kramers–Heisenberg formula and the Placzek–Teller approximation are very similar although the total cross sections differ significantly; the higher lying vibrational levels (with vibrational quantum number $v = 10\text{--}13$) are populated preferentially. When the photon energy increases to about 2.2 cm^{-1} below the resonance, the distribution predicted by the Kramers–Heisenberg equation starts to differ from the Placzek–Teller distribution; within 2.2 cm^{-1} of the resonance a significant number of lower-lying vibrational states, mainly with $v = 1\text{--}7$, become populated while the vibrational distribution predicted by the Placzek–Teller approximation remains largely unaltered. At the resonance, the Kramers–Heisenberg equation predicts no significant population of the levels with $v = 10\text{--}14$. The distribution is completely different from that predicted by the Placzek–Teller approximation which fails to take proper account of the resonance contributions. The distribution predicted by the Kramers–Heisenberg equation is similar to that obtained from consideration of spontaneous or stimulated emission from the $B^1\Sigma_u^+(v = 0, J = 1)$ state to the ground state levels.

5. Conclusion and outlook

We pointed out that molecular hydrogen may be formed by Raman scattering by a pair of hydrogen atoms colliding in the $X^1\Sigma_g^+$ state and we presented a method for the accurate evaluation of the Raman cross sections in a radiation field. We carried out a direct evaluation of the Kramers–Heisenberg equation *via* a Green operator formalism. We used a grid-based representation. We presented the first full calculation of photon-energy dependent Raman association cross sections including all rovibrational resonances associated with the intermediate states, based on the accurate electronic potential energy surfaces and properties computed by Wolniewicz and Staszewska.^{18–21} We compared the exact results with those of the Placzek–Teller approximation and we showed that

final state vibrational distributions obtained with the Placzek–Teller approximation and with the Kramers–Heisenberg expression are comparable except in the region of the resonances where they differ significantly. Future work will include thermal averaging over the collision energies of hydrogen atom pairs and calculations of Raman association rate constants with application to the formation of molecular hydrogen in astrophysical environments.

Acknowledgements

Part of this work was supported by the Institute for Theoretical Atomic, Molecular and Optical Physics at the Harvard-Smithsonian Center for Astrophysics while MvdL and MJJ visited the Institute; the Institute is supported by a grant from the National Science Foundation to Harvard University and the Smithsonian Institution. The work of AD is supported by a grant from the Chemical Sciences, Geosciences and Biosciences Division of the Office of Basic Energy Sciences, Office of Science, US Department of Energy. MvdL and GCG thank the Council for Chemical Sciences of the Netherlands Organization for Scientific Research (CW-NWO) for financial support.

References

- 1 S. Lepp, P. C. Stancil and A. Dalgarno, *J. Phys. B*, 2002, **35**, R57.
- 2 A. Dalgarno, *J. Phys.: Conference Series*, 2005, **4**, 10.
- 3 D. Galli and F. Palla, *Astron. Astrophys.*, 1998, **335**, 403.
- 4 T. Abel and Z. Haiman, *Molecular Hydrogen in Space*, Cambridge University Press, Cambridge, 1999, p. 237.
- 5 P. C. Stancil and A. Dalgarno, *Astrophys. J.*, 1997, **490**, 76.
- 6 P. C. Stancil, S. Lepp and A. Dalgarno, *Astrophys. J.*, 1998, **509**, 1.
- 7 G. Placzek and E. Teller, *Z. Phys.*, 1933, **81**, 209.
- 8 S. R. Federman and L. Frommhold, *Phys. Rev. A*, 1982, **25**, 2012.
- 9 R. Loudon, *The Quantum Theory of Light*, Oxford University Press, Oxford, 1973.
- 10 A. Dalgarno and J. T. Lewis, *Proc. R. Soc. London, Ser. A*, 1955, **233**, 70.
- 11 A. Dalgarno, A. L. Ford and J. C. Browne, *Phys. Rev. Lett.*, 1971, **27**, 1033.
- 12 A. L. Ford and J. C. Browne, *Phys. Rev. A*, 1973, **7**, 418.
- 13 M. Marinescu, H. R. Sadeghpour and A. Dalgarno, *J. Opt. Soc. Am. B*, 1993, **10**, 988.
- 14 I. Simbotin, M. Marinescu, H. R. Sadeghpour and A. Dalgarno, *J. Chem. Phys.*, 1997, **107**, 7057.
- 15 I. Simbotin, M. J. Jamieson and A. Dalgarno, *J. Geophys. Res., [Atmos.]*, 2004, **109**, D13302.
- 16 M. C. G. N. van Vroonhoven and G. C. Groenenboom, *J. Chem. Phys.*, 2002, **116**, 1965.
- 17 D. T. Colbert and W. H. Miller, *J. Chem. Phys.*, 1992, **96**, 1982.
- 18 L. Wolniewicz and G. Staszewska, *J. Mol. Spectrosc.*, 2002, **212**, 208.
- 19 L. Wolniewicz and G. Staszewska, *J. Mol. Spectrosc.*, 2003, **217**, 181.
- 20 L. Wolniewicz and G. Staszewska, *J. Mol. Spectrosc.*, 2003, **220**, 45.
- 21 L. Wolniewicz, *J. Chem. Phys.*, 2004, **1851**, 99.
- 22 U. Fantz and Wunderlich, IAEA report INDC(NDS)-457, 2004. Available online via <http://www-amdis.iaea.org>. The calculations are based on the same *ab initio* data as the current work.
- 23 T. Seideman and W. H. Miller, *J. Chem. Phys.*, 1992, **96**, 4412.
- 24 T. Seideman and W. H. Miller, *J. Chem. Phys.*, 1992, **97**, 2499.
- 25 T. Seideman, *J. Chem. Phys.*, 1993, **98**, 1989.